Palb2 synergizes with *Trp53* to suppress mammary tumor formation in a model of inherited breast cancer

Christian Bowman-Colin[a], Bing Xia[b], Samuel Bunting[c], Christiaan Klijn[d,1], Rinske Drost[d], Peter Bouwman[d], Laura Fineman[a], Xixi Chen[a], Aedin C. Culhane[e,f], Hong Cai[b], Scott J. Rodig[g], Roderick T. Bronson[h], Jos Jonkers[d], Andre Nussenzweig[i], Chryssa Kanellopoulou[a,2,3], and David M. Livingston[a,3]

[a]Department of Cancer Biology, and [e]Biostatistics and Computational Biology, Dana-Farber Cancer Institute, Boston, MA 02215; [b]Cancer Institute of New Jersey, New Brunswick, NJ 08901; [c]Department of Molecular Biology and Biochemistry, Rutgers University, Piscataway, NJ 08854; [d]Division of Molecular Pathology, The Netherlands Cancer Institute, 1066 CX Amsterdam, The Netherlands; [f]Biostatistics, Harvard School of Public Health, Boston, MA 02115; [g]Department of Pathology, Brigham and Women's Hospital, Boston, MA 02115; [h]Rodent Histology Core, Dana-Farber/Harvard Cancer Center, Harvard Medical School, Boston, MA 02115; and [i]Laboratory of Genome Integrity, National Cancer Institute, National Institutes of Health, Bethesda, MD 20892

Germ-line mutations in *PALB2* lead to a familial predisposition to breast and pancreatic cancer or to Fanconi Anemia subtype N. PALB2 performs its tumor suppressor role, at least in part, by supporting homologous recombination-type double strand break repair (HR-DSBR) through physical interactions with BRCA1, BRCA2, and RAD51. To further understand the mechanisms underlying PALB2-mediated DNA repair and tumor suppression functions, we targeted *Palb2* in the mouse. *Palb2*-deficient murine ES cells recapitulated DNA damage defects caused by PALB2 depletion in human cells, and germ-line deletion of *Palb2* led to early embryonic lethality. Somatic deletion of *Palb2* driven by *K14*-Cre led to mammary tumor formation with long latency. Codeletion of both *Palb2* and Tumor protein 53 (*Trp53*) accelerated mammary tumor formation. Like *BRCA1* and *BRCA2* mutant breast cancers, these tumors were defective in RAD51 focus formation, reflecting a defect in *Palb2* HR-DSBR function, a strongly suspected contributor to *Brca1*, *Brca2*, and *Palb2* mammary tumor development. However, unlike the case of *Brca1*-mutant cells, *Trp53bp1* deletion failed to rescue the genomic instability of *Palb2*- or *Brca2*-mutant primary lymphocytes. Therefore, *Palb2*-driven DNA damage control is, in part, distinct from that executed by *Brca1* and more similar to that of *Brca2*. The mechanisms underlying *Palb2* mammary tumor suppression functions can now be explored genetically in vivo.

mouse model | familial breast cancer

Partner and Localizer of BRCA2 (*PALB2*) is a breast cancer susceptibility gene. Its product was identified as a major interacting protein of the BReast CAncer susceptibility gene product 2, BRCA2 (1). This interaction is required for the repair of DNA double strand breaks (DSBs) by homologous recombination (HR) because PALB2 is necessary for the chromatin association of BRCA2 and its partner, RAD51 (1). RAD51 is the central recombinase in HR, and it participates in D-loop formation and strand displacement (2). PALB2 also plays a BRCA2-independent role in the HR process by enhancing RAD51 function (3, 4).

PALB2 interacts with both BRCA1 and BRCA2 and mediates the long-known interaction between these proteins (5, 6). Loss of PALB2 does not affect BRCA1 recruitment to irradiation-induced foci (IRIF) but abrogates colocalization of BRCA2 and RAD51 at these structures (1, 5). Genetic analyses have shown that, like BRCA2, a member of Fanconi anemia complementation group D1, PALB2 is also the Fanconi anemia complementation group N protein (FANCN) (7, 8). PALB2 is also a breast cancer suppressor protein in its own right (9–12). Unlike *BRCA1* and *BRCA2* mutant tumors, only some *PALB2*-associated breast cancers have undergone loss of *PALB2* heterozygosity (LOH) (9, 10). This finding implies that a reduction of *PALB2* gene copy number might be sufficient to allow breast cancer development in some, but not all, settings. Why this difference exists is an open question.

Breast cancer in *PALB2*-mutated families is of intermediate penetrance, unlike that in *BRCA1/2* families (10, 12). Although

PALB2 mutations are rarer than *BRCA1/2* mutations, available clinical data suggest that heterozygous, germ-line *PALB2* mutations do not precisely phenocopy either *BRCA1* or *BRCA2* cancer predisposition syndromes (9, 10). This finding is consistent with the notion that PALB2 biological functions extend beyond simply enabling BRCA1–BRCA2 complex formation. PALB2 also interacts with MRG15 (also known as MORF4L1) (13), a subunit of histone acetyl transferase/deacetylase complexes, and with KEAP1, a major regulator of the antioxidant transcription factor NRF2 (also known as NFE2L2) (14). In addition, PALB2 contains a highly conserved, chromatin-associated domain (ChAM) for which no binding partners are known (15). The contribution of these PALB2 binding partners and of the ChAM domain to the BRCA1-PALB2-BRCA2 HR machinery and/or to PALB2's cancer suppression function is unclear. Thus, it is conceivable that PALB2 exerts multiple functions that extend beyond its known role in HR-mediated double strand break repair.

To date, it has been difficult to study the molecular pathogenesis of *PALB2* breast cancer in detail because of the lack of a genetically engineered mouse model that recapitulates the human disease. Thus, we have generated a model of *Palb2* breast cancer in the mouse and have documented its most salient properties. An analogous model was recently generated by others (16).

Results and Discussion

Targeting the Mouse *Palb2* Gene and Generation of *Palb2*-Deficient ES Cells. To generate a *Palb2* allele that could be conditionally inactivated upon Cre recombinase expression, we inserted *loxP* sites flanking exons 2 and 3 of the *Palb2* gene (Fig. S1 *A* and *B*). These exons encode a putative nuclear localization signal sequence and the PALB2 coiled-coil domain (Fig. 1*A*, Fig. S1*A*). The latter mediates the PALB2 interaction with BRCA1 (5, 6). Deletion of these exons would result in out-of-frame reading of exon 4 and premature termination of the PALB2 translation before the BRCA2-interacting, seven-bladed WD40-type β-propeller domain (Fig. 1*A*, Fig. S1*A*). Due to premature truncation
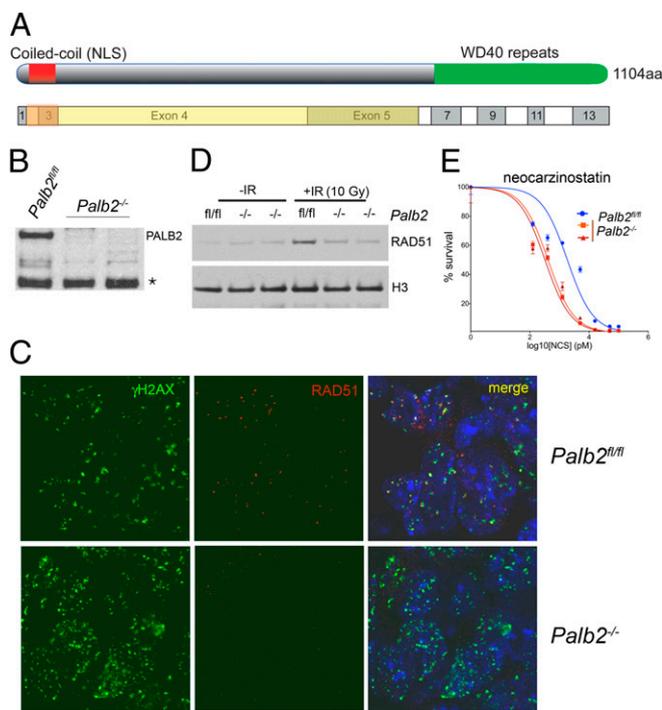
Fig. 1. Conditional gene targeting of mouse *Palb2*. (*A*) Schematic representation of *Palb2* domains and the exons from which they are encoded. The yellow area corresponds to the frameshifted ORF that results from recombination of the inserted *loxP* recombination sites. (*B*) Western blot analysis for PALB2 isolated in chromatin-enriched extracts (S420) of three independent ES cell lines. The full-length mouse PALB2 protein is ~120 kDa. A nonspecific background band is indicated by an asterisk and can be used as an internal loading control. (*C*) Recruitment of RAD51 to DSBs marked by γH2AX IRIF 2 h after exposure of *Palb2^fl/fl* and *Palb2^−/−* ES cells to to 5 Gy of ionizing radiation (IR). (*D*) Western blot analysis of chromatin-bound (S420) RAD51 in *Palb2^fl/fl* and *Palb2^−/−* ES cells that received 10 Gy of IR and the respective unirradiated control cells. Histone H3 was used as a loading control. (*E*) Dose–response curves of *Palb2^fl/fl* and *Palb2^−/−* ES cells after exposure to increasing concentrations of neocarzinostatin.

of the *Palb2* ORF, the resulting transcript is also a candidate for degradation via nonsense-mediated decay.

Targeting of the *Palb2* locus and integration of both *loxP* recombination sites was confirmed by Southern blot analysis (Fig. S1C). Heterozygous ES cells (*Palb2*^neo/+) were injected into blastocysts, and the resulting chimeras from two individual clones were bred to either *Flp*-deleter mice (to eliminate the Frt-flanked neomycin resistance cassette and generate a conditional allele) or *Cre*-deleter mice (to generate a conventional *Palb2* KO allele). Germ-line transmission of the *Palb2*^neo allele occurred from nearly all chimeras, and mice were successfully genotyped for the Flp- and the Cre-recombined alleles (*Palb2^fl* or *Palb2^−*, respectively).

We attempted to derive ES cells from the *Palb2^−* allele. Three, independent *Palb2* ES cell lines were derived from a single, heterozygous *Palb2^fl/−* cross. Expression analysis of *Palb2* mRNA by quantitative real-time RT-PCR (qRT-PCR) confirmed that one of these ES lines was *Palb2^fl/fl* and the other two were *Palb2^−/−* (Fig. S1D). The loss of full-length Palb2 expression from these lines was further confirmed by Western blotting, using a polyclonal anti-mouse PALB2 antibody raised against the N-terminal 200 residues of the mouse PALB2 protein (Fig. 1B). Therefore, *Palb2* loss did not prevent ES cell derivation and subsequent survival. The three ES cell lines we derived were morphologically comparable, proliferated at the same rate as wild-type (WT) ES cells and were capable of differentiation into embryoid bodies.

ES cells that are deficient for *Brca1* or *Brca2* have been notoriously difficult to isolate and are severely compromised in their proliferation (17, 18). In keeping with these findings, *Palb2^−/−* ES cells could not be derived from embryos carrying a conventional PALB2 gene-trap allele (19). Because PALB2 operates immediately upstream of BRCA2 and is required for BRCA2 localization at DNA double strand breaks, it is possible that the viability and robustness of our *Palb2^−/−* ES cells were due to residual expression of a truncated PALB2 species. Such a polypeptide could, in theory, result from translation initiation downstream of the engineered *Palb2* genomic deletion. No such truncated protein was detected with our polyclonal antibody (Fig. 1B).

To test whether the conditional gene targeting approach that was used had generated an allele that would be rendered null after Cre action, the response of *Palb2^fl/fl* and *Palb2^−/−* ES cells to DNA damaging agents that cause double strand breaks was analyzed. Normally, exposure of *PALB2*-proficient cells to ionizing radiation (IR) leads to the formation of phosphorylated histone H2A.X (γH2AX) nuclear foci and subsequent recruitment of BRCA1, BRCA2, and RAD51 to these structures. As expected, after exposure to IR, γH2AX and BRCA1 IRIF formation was unaffected in *Palb2^−/−* cells (Fig. 1C, Fig. S2A). However, the recruitment of RAD51 was severely compromised (Fig. 1C). This defect was also evident at the biochemical level because no increase in chromatin loading of RAD51 after IR could be detected in nuclear extracts of IR-treated *Palb2^−/−* cells (Fig. 1D).

Because biallelic PALB2 mutations in humans cause Fanconi anemia, a hallmark of which is increased sensitivity to DNA cross-linking agents such as mitomycin C (MMC), the sensitivity of *Palb2^−/−* ES cells to MMC as well other DNA damaging agents was assayed. Both *Palb2^−/−* ES lines displayed increased sensitivity to MMC, IR, and the radiomimetic drug, neocarzinostatin (Fig. 1E, Fig. S2 *B* and *C*). These findings further imply that these *Palb2^−/−* cells are functional KOs for *Palb2* because they are compromised in multiple, known *Palb2*-associated functions. Thus, upon Cre-mediated recombination in vivo, the aforementioned conditional *Palb2* allele appears to be converted to a *Palb2*-null allele.

Loss of *Palb2* in the Germ Line Results in Early Embryonic Lethality.
Germ-line deletion of *Brca1* or *Brca2* results in early embryonic lethality (17, 20, 21). Although *Palb2^−/−* ES cells displayed no apparent growth defects compared with *Palb2^fl/fl* controls, *Palb2* loss could still be deleterious in differentiated progeny cells, and thereby negatively affect mouse development. Indeed, we were unable to obtain *Palb2^−/−* mice from heterozygous crosses (Fig. S3A), consistent with previous reports (19, 22). Dissection of embryos from timed pregnancies revealed that *Palb2*-null embryos could be recovered only up to E12.5, but even then at sub-Mendelian ratios. These embryos repeatedly exhibited severe malformations. At earlier time points, morphological aberrations of *Palb2^−/−* embryos were less obvious. However, these mutant embryos were clearly smaller than WT or heterozygous littermate embryos (Fig. S3B), and some displayed exencephaly as well as malformations of the placental labyrinth and yolk sac-associated blood islets (Fig. S3 *C–F*). The fact that *Palb2* nullizygosity resulted in embryonic lethality detectable at E8.5–E10.5 is consistent with earlier reports showing that homozygous *Palb2*-deficient mice also die during embryogenesis at ~E8.5 (19, 22).

Embryonic lethality due to loss of *Brca1* or *Brca2* can be delayed by concomitant loss of P53 (encoded by *Trp53*) or the CDK inhibitor p21 (encoded by the *Cdkn1a* gene) (23), (24). *Trp53* loss also delayed the lethality of *Palb2* KO embryos, which otherwise exhibited increased p21 abundance (22). We therefore tested whether loss of p21 expression affects *Palb2^−/−* embryonic lethality by generating *Palb2*; *Cdkn1a^−/−* embryos. As expected, loss of p21 expression did delay embryonic lethality of *Palb2* KO embryos by 2–3 d (Fig. S3A). However, all *Palb2/Cdkn1a* double KO embryos still displayed multiple malformations and impaired growth compared with *Palb2* heterozygous or WT littermates

GENETICS

and were eventually resorbed. Therefore, these $Palb2^{-/-}$ embryonic rescue effects were incomplete and failed to suppress embryonic lethality.

Because the establishment of the placenta and onset of embryonic hematopoiesis are critical steps in development that take place around the time of lethality of $Palb2$ embryos, we asked whether the lethality of $Palb2$ KO embryos could be bypassed by a WT placenta. To this end, we used the $Palb2^{fl/fl}$ and $Palb2^{-/-}$ ES cells we had generated to perform tetraploid complementation assays. In this assay, diploid KO ES cells are aggregated to tetraploid WT blastocysts to generate KO embryos that are supported by a WT placenta because the tetraploid WT blastomeres are still capable of forming a placenta but cannot contribute to the embryo.

We found that embryos derived from the $Palb2^{-/-}$ ES cells were already underdeveloped and malformed at E9.5 compared with their $Palb2^{fl/fl}$ counterparts (Fig. S3 *I and J*). At E12.5, embryos derived from $Palb2^{fl/fl}$ ES cells appeared normal whereas embryos from $Palb2^{-/-}$ ES cells had been resorbed (Fig. S3 *K and L*). Likewise, breeding of the $Palb2^{fl/fl}$ conditional allele to *Meox2-Cre* knock-in (KI) mice (in which Cre is expressed from the endogenous *Meox2* locus only in the embryo proper and not in the placenta or extraembryonic tissues) (25) only yielded viable mice in which the $Palb2$ deletion was incomplete. Collectively, these findings indicate that $Palb2$ is an essential gene during development, and its deficiency in the embryo proper is incompatible with life. These findings are analogous to previous results showing that the lethality of $Brca1^{-/-}$ embryos could not be rescued by tetraploid complementation assay (20).

Palb2 Is a Breast Tumor Suppressor in Mice.

To assess the effect of *Palb2* loss-of-function on mammary tumorigenesis, we crossed $Palb2^{fl/fl}$ mice with keratin 14 promoter-driven *Cre* (*K14-Cre*) transgenic mice (26). *K14-Cre* transgenic animals preferentially express Cre recombinase in the basal epithelium of the mammary ducts, as well as in skin and oral mucosa. *K14-Cre* has previously been used to model murine *Brca1* and *Brca2* mammary tumorigenesis (27).

PALB2, like BRCA1 and -2, appears to be a breast cancer suppressor in humans (9, 10, 28). Therefore, in an effort to develop a tractable system for studying how *Palb2* operates in this regard, we set out to develop a *Palb2* mouse breast cancer model. Mammary tumor formation initiated by BRCA1 or BRCA2 loss requires concomitant loss of functional p53 (encoded by *Trp53* in mice) (27, 29). This observation was considered in efforts to establish a *Palb2* model.

We first generated *Palb2/Trp53* double conditional mice by crossing $Palb2^{fl/fl}$; *K14-Cre* transgenic mice with *Trp53* conditional mice. All mice that harbored the conditional alleles for *Palb2* and/or *Trp53* in the absence of *K14-Cre* were phenotypically normal, fertile, and capable of nursing their litters. During the period of tumor monitoring (up to 600 d after birth), $Trp53^{fl/fl}$; *K14-Cre* female mice developed spontaneous mammary tumors with a frequency of ~80% and a mean tumor-free interval ($T_{1/2}$) of 320 d. By contrast, $Palb2^{fl/fl}$; $Trp53^{fl/fl}$; *K14-Cre* double conditional mice developed tumors much faster ($T_{1/2}$ = 192 d, $P = 2.4 \times 10^{-5}$), indicating that *Palb2* loss accelerates tumor formation on a *Trp53*-null background (Fig. 2*A*). These latencies are comparable with $Brca2^{fl/fl}$; $Trp53^{fl/fl}$; *K14-Cre* and $Brca1^{fl/fl}$; $Trp53^{fl/fl}$; *K14-Cre* mice ($T_{1/2}$ = 181 and 213 d, respectively) (27, 30).

Somatic loss of one *Trp53* allele displayed, as expected, a haploinsufficient tumor suppressor phenotype (27, 30), given that $Palb2^{fl/fl}$; $Trp53^{fl/+}$; *K14-Cre* mice developed tumors significantly faster than $Palb2^{fl/fl}$; $Trp53^{+/+}$; *K14-Cre* mice ($T_{1/2}$ = 225 d vs. 420 d, respectively, $P = 2.5 \times 10^{-12}$, Fig. S4*C*). *Palb2* loss of function also accelerated tumor formation on a *Trp53* heterozygous (fl/+) background, again reflecting the genetic interaction of these two genes (Fig. 2*B*).
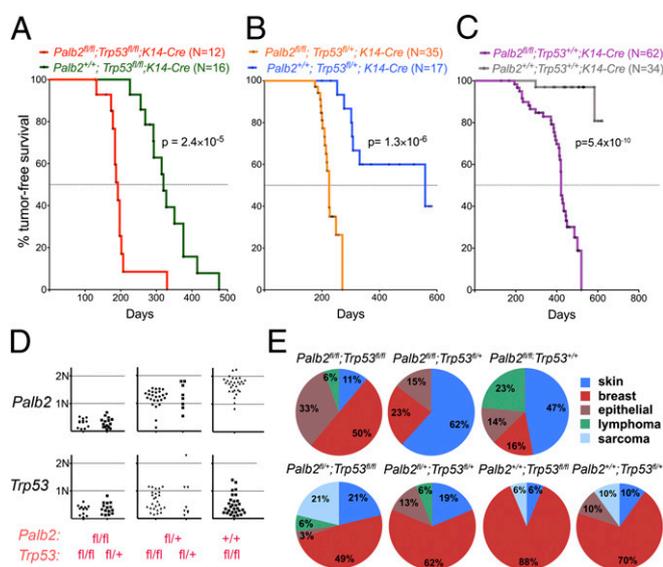

Fig. 2. Tumor formation in $Palb2^{fl/fl}$ conditional mice. (*A–C*) Kaplan–Meier curves display that *Palb2* loss accelerates tumor formation both on a *Trp53*-conditional null background (*A*), on a *Trp53*-conditional heterozygous background (*B*), and on a *Trp53* WT background (*C*). (*D*) Gene dosages of *Palb2* (*Upper*) and *Trp53* (*Lower*) in mammary tumors derived from *Palb2/Trp53* double conditional mouse cohorts. The germ-line *Palb2* and *Trp53* genotypes of the mice are indicated in red below the graphs. (*E*) Spectrum of tumors arising in mouse cohorts with different combinations of *Palb2* and *Trp53* alleles. The genotypes of the mice are shown above the graphs.

K14-Cre-mediated loss of *Palb2* and *Trp53* led, predominantly, to tumor formation in breast, skin, and oral mucosa (Fig. 2*E*), as previously reported for *K14-Cre*-driven *Brca1* and *Brca2* cancers (27, 30–32). All of the mammary cancers were estrogen and progesterone receptor (ER/PR)-negative, basal-like (Fig. S4 *D–F*), much like the BRCA1 and -2 tumors generated by *K14-Cre* (30, 32). Although most of the tumors found in $Palb2^{+/+}$; $Trp53^{fl/fl}$; *K14-Cre* mice were breast carcinomas, *Palb2/Trp53* compound KO mice displayed an expanded spectrum of tissues affected by tumors (Fig. 2*E*), suggesting that combined loss of PALB2 and P53, possibly due to some expression of Cre in other tissues, also results in tumor formation that is not restricted to the mammary gland.

Mice harboring conditional alleles for *Palb2* and *Trp53*, but no *K14-Cre* transgene, and $Palb2^{+/+}$; $Trp53^{+/+}$; *K14-Cre* mice did not display overt tumor formation during the observation period (Fig. 2*C*), despite the intrinsic mutagenic activity of Cre in mammalian cells (31, 33). Therefore, tumor formation in the above-noted experiments is a product of targeted gene deletion.

All tumors from $Palb2^{fl/fl}$; $Trp53^{fl/fl}$; *K14-Cre* mice (*n* = 12) had lost both copies of *Palb2* and *Trp53* (Fig. 2*D*). Similarly, in all tumors from $Palb2^{fl/fl}$; $Trp53^{fl/+}$; *K14-Cre* mice (*n* = 15), the conditional *Palb2* and *Trp53* alleles were recombined. The WT copy of *Trp53* was also lost in most tumors, probably through LOH.

Early reports describing a lack of *PALB2* LOH in clinical tumor samples from heterozygous patients suggested that PALB2 could be a haploinsufficient tumor suppressor in humans whereas other reports showed that multiple *PALB2* tumors revealed *PALB2* LOH, implying that the *PALB2* tumor formation process is not uniform (9, 34, 35). In our experimental setting, no haploinsufficiency for tumor suppression was observed for *Palb2*, as indicated by the comparable latency in $Palb2^{fl/+}$; $Trp53^{fl/fl}$; *K14-Cre* and $Palb2^{+/+}$; $Trp53^{fl/fl}$; *K14-Cre* tumor development ($P = 0.46$, Fig. S4*A*). Similarly, when compared on a $Trp53^{fl/+}$; *K14-Cre* background, cohorts of $Palb2^{+/+}$ and $Palb2^{fl/+}$ mice developed tumors with similar latency and frequency ($P =$

0.96, Fig. S4B), implying that heterozygous *Palb2* loss of function did not contribute to tumor formation.

Moreover, *Palb2* heterozygous mouse breast tumor lines displayed proper RAD51 localization at IRIF, consistent with preserved HR function (see Fig. 4C). By contrast, *Palb2*$^{-/-}$ breast tumor cell lines displayed the same defect in RAD51 accumulation observed in *Palb2*-null primary cells (see Fig. 4C). These findings suggest a role for HR deficiency in the genesis of *Palb2* tumors, a state that is not compatible with retention of a functional copy of the gene. Moreover, an analysis of tumors that arose in *Palb2*$^{fl/+}$; *Trp53*$^{fl/fl}$; *K14-Cre* mice implies that a significant fraction of these tumors retained at least one copy of *PALB2*, suggesting that loss of one copy of the gene did not contribute to tumor formation in this model (Fig. 2D).

Although we observed long latency tumors only in *Palb2*$^{fl/fl}$; *K14-Cre* mice on a WT *Trp53* background (T$_{1/2}$ = 420 d), tumor formation was nonetheless highly significant compared with *Palb2*$^{+/+}$; *Trp53*$^{+/+}$; *K14-Cre* controls ($P = 5.4 \times 10^{-10}$, Fig. 2C). The majority of these tumors were small lesions in the head and neck, and a few were mammary tumors. All of these mammary tumors were *Palb2*$^{-/-}$, and all displayed either mutations in or loss of *Trp53* by LOH.

The finding that loss of *Palb2* alone is sufficient to induce long latency tumor formation contrasts with most *Brca1* and *Brca2* mouse models in which significant numbers of these tumors could not be detected, unless *Trp53* was codeleted (27, 30, 36, 37). One explanation for this finding is that somatic *Palb2* loss might be better tolerated than somatic *Brca1/2* loss on a *Trp53* WT background. This hypothesis fits with the finding that *Palb2* nullizygosity gives rise to a less severe phenotype in ES cells than biallelic *Brca1* or *Brca2* loss (17, 18, 27, 38).

Genomic Features of *Palb2*/*Trp53*-Deficient Mammary Tumors. Genomic instability is a hallmark of human cancer, and it promotes tumor initiation and progression. Experimental mouse tumor models have recapitulated this aspect of human tumorigenesis (39). To gain insight into the genomic structures of the tumors that arose due to the loss of *Palb2*, we performed high-resolution comparative genomic hybridization (CGH) (40) analysis of *Palb2*/*Trp53*, *Brca1*/*Trp53*, *Brca2*/*Trp53*, and *Trp53* only-deficient mammary tumors that arose in *K14-Cre* mice (Fig. 3 A–C).

Segmentation analysis of the CGH data was performed for each tumor to assess the number of genomic segments with deviating copy number changes (aka genomic segmentation), as a readout of genomic instability (41). *Palb2*/*Trp53* and *Brca1*/*Trp53* tumors displayed apparently greater genomic instability (genomic segmentation) compared with *Brca2*/*Trp53* and *Trp53*-only tumors, but the difference was not statistically significant. However, when the relative dose of amplified segments (log$_2$ dose ≥ 0.5) was analyzed, *Palb2*/*Trp53* mammary tumors ($n = 8$) displayed a significantly higher average dose of amplified segments than either *Brca1*/*Trp53* ($n = 4$; $P < 0.0001$, Fig. 3C) or *Brca2*/*Trp53* tumors ($n = 5$; $P = 0.0014$, Fig. 3C). The low numbers of deletions (log$_2$ dose ≤ -0.5) detected in *Brca2*/*Trp53* and *Trp53*-only tumors precluded further analysis of this aspect of genomic instability (Fig. 3B).

No significant difference in focal genome amplification appeared when *Palb2*/*Trp53* tumors were compared with *Trp53*-only tumors, indicating that *Palb2*/*Trp53* tumors share a similar amplification-prone genomic profile with *Trp53*-only tumors, despite their marked difference in tumor formation kinetics. The inability of *Palb2* loss to suppress focal genomic amplifications (unlike what was observed in *Brca1*/*Trp53* and *Brca2*/*Trp53* tumors) could be accounted for by three, alternative explanations.

First, these differences could be due to residual activity of the conditional *Palb2* allele we generated, and other *Palb2* loss of function mutations might trigger the formation of true *Brca2* tumor phenocopies. Second, our allele is a functional null, as our
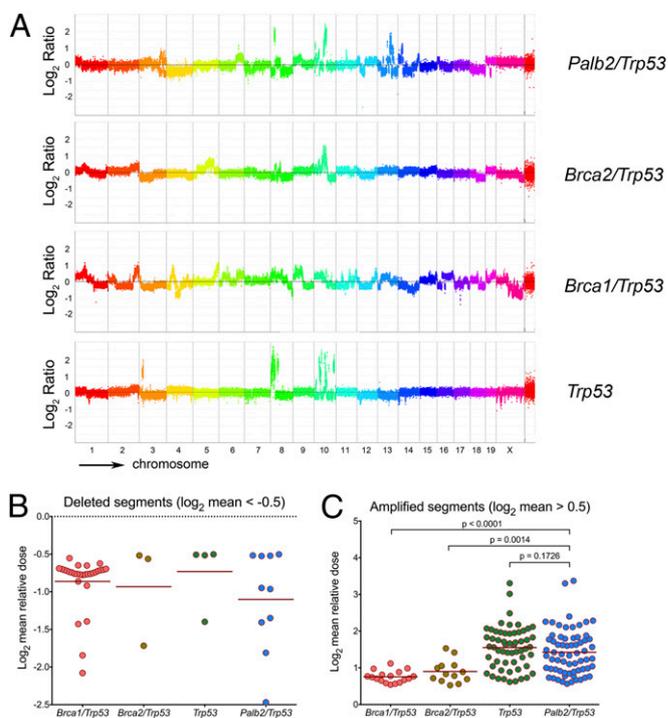

Fig. 3. CGH analysis of *Palb2* tumors. (A) Control (spleen) and tumor DNAs were hybridized to whole genome arrays to determine regions of loss or gains in mouse breast tumor samples. Representative rainbow graphs for each tumor genotype showing log$_2$ mean DNA relative dose ratio (tumor/spleen) across the entire genome are presented. Each dot represents the average signal from 10 or more consecutive probes (or a segment of ~40 kb of genomic DNA). The amplitude of the data points above or below the midline indicates the extent of loss/gain in each segment, respectively. (B and C) Scatter plot graphs indicating the relative dose of the deleted segments (log$_2$ < −0.5, B) and amplified segments (log$_2$ > 0.5, C), each dot representing one segment. The number of dots represents the number of segments for all tumors of the relevant genotype, and the number of tumors analyzed (n) for *Brca1*/*Trp53*, *Brca2*/*Trp53*, *Trp53*-only, and *Palb2*/*Trp53* tumors were 4, 5, 7, and 8, respectively. The horizontal lines are the average segment dose per genotype, and the P values displayed correspond to the result of the nonparametric Mann–Whitney–Wilcoxon signed-rank test, which followed the Kruskal–Wallis one-way analysis of variance ($P < 0.0001$).

studies suggest, but complete loss of *Palb2* is similar to a BRCA2 hypomorphic phenotype rather than a complete loss of BRCA2 function. Alternatively, there are PALB2 functions that are, at least in part, nonoverlapping with the tumor suppressing functions of its BRCA2 partner protein. New experiments with additional *Palb2* and *Brca2* mutant mouse strains would be required to distinguish between these possibilities.

Finally, tumor heterogeneity likely affected the CGH profiles (Fig. S5) in ways that make it difficult to identify regions of chromosomal imbalances that were unique to *Palb2*/*Trp53* tumors. Conceivably, a more comprehensive analysis with a much larger collection of tumor samples would reveal such regions.

Loss of 53BP1 Fails to Rescue the HR Defect Caused by PALB2 Deficiency. Loss of 53BP1 can rescue the HR defect and lethality observed in either *Brca1*$^{\Delta11/\Delta11}$ or *Brca1*-null cells and mice (42–45). Similarly, decreased expression of the P53 binding protein 1 (53BP1) was detected in triple negative breast cancers as well as human *BRCA1* tumors (45). Therefore, we asked whether *Trp53bp1* (which encodes mouse 53BP1) expression is reduced in *Palb2*/*Trp53* KO tumors, and whether its absence rescues the HR defect associated with *Palb2* loss. Quantitative RT-PCR analysis of *Trp53bp1* mRNA in freshly isolated *Palb2* breast tumor samples
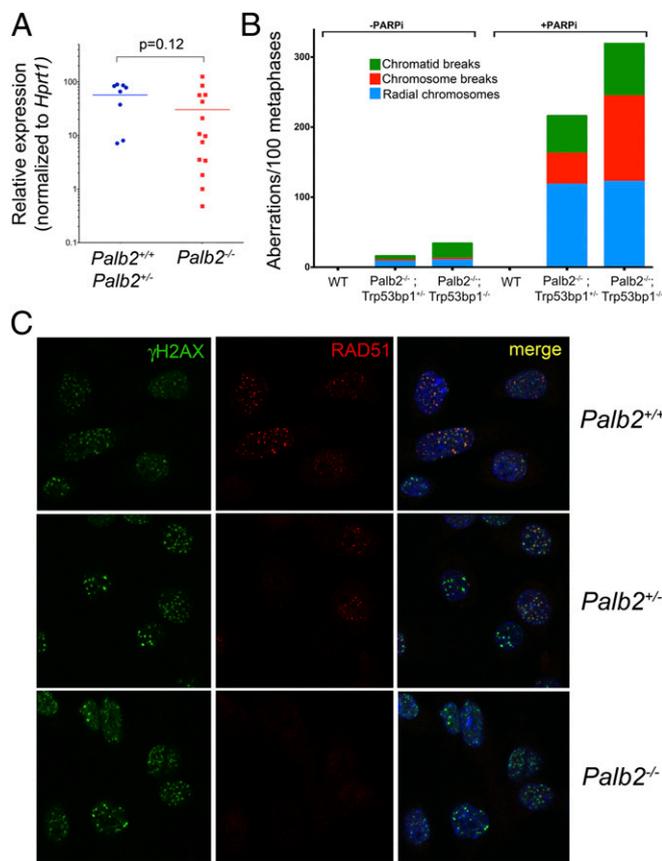
GENETICS

Fig. 4. The HR defect in *Palb2*-deficient cells and tumors. (*A*) qRT-PCR for *Trp53bp1* mRNA in freshly isolated tumor samples that are either *Palb2*-proficient (+/+ and +/−, n = 8) or *Palb2*-deficient (−/−, n = 14). Horizontal lines represent the average relative expression value and the *P* value associated to this comparison (Mann–Whitney *U* test) is indicated. (*B*) Acute chromosomal damage and genome instability observed in chromosome spreads following PARPi treatment that are not rescued by *Trp53bp1* deletion in *Palb2^{fl/fl}*;*CD19-Cre* B lymphocytes. (*C*) Established *Palb2/Trp53*-deficient breast tumor cell lines (example shown in the *Bottom* panels) reveal a defect in the recruitment of RAD51 to IRIF whereas *Palb2* heterozygosity does not impair the proper IRIF localization of RAD51 in breast tumor lines (*Middle* panels). Both should be compared with a *Palb2* WT control breast tumor line (*Top* panels).

showed that levels of *Trp53bp1* messenger varied considerably among the tumors that were analyzed. However, overall *Trp53bp1* mRNA levels were not significantly different in *Palb2*-deficient and *Palb2*-proficient tumors (Fig. 4*A*).

To determine whether HR deficiency due to *Palb2* loss is complemented by *Trp53bp1* loss in primary cells (cultured primary splenic B cells), we generated *Palb2^{fl/fl}*; *CD19-Cre* mice that were or were not deficient in *Trp53bp1*. Cultured primary splenocytes from these mice were then assayed for HR competence upon treatment with PARP inhibitors (PARPi), which selectively induces DNA damage and chromosomal aberrations in HR-deficient cells (46). Treatment with KU0058948 (PARPi) led to an accumulation of chromosomal and chromatid breaks, and radial structures were evident in chromosomal spreads from cultured *Palb2^{fl/fl}*; *Trp53bp1^{+/−}*; *CD19-Cre* primary splenocytes (Fig. 4*B*). The number of chromosomal aberrations observed was not reduced in *Palb2^{fl/fl}*; *Trp53bp1^{−/−}*; *CD19-Cre* splenocytes, implying that *Trp53bp1* deletion did not complement the HR defect caused by *Palb2* deficiency (Fig. 4*B*). *Trp53bp1* deletion also failed to rescue the chromosomal aberrations found in spreads from PARPi-treated *Brca2^{fl/fl}*; *Trp53bp1^{−/−}*; *CD19-Cre* splenocytes (Fig. S6*A*),

which appeared to be even more extensive than those observed in PARPi-treated *Palb2^{fl/fl}*; *Trp53bp1^{−/−}*; *CD19-Cre* cells (Fig. 4*B*). As has been previously described (43, 45), complete rescue of the DNA repair deficiency in *Brca1^{fl/fl}*; *Trp53bp1^{−/−}*; *CD19-Cre* splenocytes was observed (Fig. S6*B*).

Of note, both *Palb2/Trp53bp1* and *Brca2/Trp53bp1* compound KO cells displayed more chromosomal aberrations after PARPi exposure than *Palb2* or *Brca2* single mutants (Fig. 4*B*, Fig. S6*A*). Thus, whereas *Brca1, Palb2,* and *Brca2* manifest closely related, even overlapping functions, loss of *Palb2* or *Brca2* also resulted in a different DNA damage response after *Trp53bp1* elimination from that manifested by *Brca1* KO cells, in which *Trp53bp1* codeletion rescued the genomic instability observed after PARP inhibition.

These observations suggest that the contributions of PALB2 and BRCA2 to HR-based DSB repair are distinct from those of BRCA1 and cannot be complemented by 53BP1 loss. In keeping with existing evidence, PALB2 and BRCA2 may be de facto HR effectors that cannot be replaced or bypassed, except by artificially forcing the loading of RAD51 onto chromatin at/near DSB, which 53BP1 loss has not yet been shown to promote (45, 47–49). These observations, along with earlier results (4), also suggest that PARP inhibition might be a potential therapeutic regimen in PALB2-deficient tumors, as it is in BRCA1- and BRCA2-associated tumors (46).

Conclusions

In summary, we have shown that *Palb2* is a breast tumor suppressor gene in mice as it is in humans and that it synergizes with *Trp53* to suppress tumor formation. The outcome of dual *Palb2/Trp53* nullizygosity in the mouse mammary gland is highly penetrant breast cancer. In keeping with the fact that *PALB2* is also a breast tumor suppressor in humans, *PALB2* might be viewed as a *BRCA3*-like allele. Moreover, tumorigenesis driven by *Palb2* loss in the mouse is not entirely suppressed on a *Trp53* WT germline background, unlike most *Brca1* and *Brca2* mouse models of breast tumorigenesis (50).

Despite many similarities to *Brca2/Trp53* and *Brca1/Trp53* breast tumors, *Palb2* tumors displayed certain divergent genomic features that might be viewed as separating them from BRCA1 and -2 cancers. Specifically, we observed patterns of genomic aberrations that were different in *Palb2/Trp53*-derived tumors from those detected in *Brca1/Trp53*- or *Brca2/Trp53*-derived tumors. These data are consistent with the hypothesis that PALB2 possesses biological functions that extend beyond those of its major interactors, BRCA1 and BRCA2. Alternatively, the effect of *Palb2* deletion may mimic a phenotype akin to partial loss of BRCA2, resulting in a less dramatic genomic instability profile in the relevant tumor cells.

Although the genomic instability of *Brca1*-deficient cells can be rescued by loss of *Trp53bp1*, deletion of the latter had, if anything, an adverse effect in *Palb2* KO cells. In that context, *Palb2* is more similar to *Brca2*, the absence of which leads to an HR defect that also cannot be rescued by *Trp53bp1* deletion.

Haploinsufficiency for *Palb2* tumor suppression was not detected in this model although one cannot rule out the possibility that it would be manifest in a different model system and/or with enlarged cohorts of experimental mice. For example, the tumors in this mouse model driven by *K14-Cre* were uniformly of the triple negative phenotype. This characteristic might well contribute to the absence of haploinsufficiency in our system, in the same way that BRCA1 mammary tumors derived from distinct cell populations display preferential patterns of consecutive LOH events along the tumorigenesis pathway (32, 51).

We believe that this mouse model will be useful in understanding how *Palb2* serves its breast cancer suppression function.

Materials and Methods

ES Cell Derivation, Embryo Harvesting, and Tetraploid Complementation Assay.
Generation of the conditional allele for *Palb2* and additional experimental details are described in *SI Material and Methods.* Oligo sequences used are described in Table S1. ES cell derivation was performed according to standard protocols (52). Pregnant mice from timed matings were killed at indicated time points by CO_2 asphyxiation following institutional guidelines. Uterine horns and embryos were dissected under the microscope, and isolated embryos were directly used for digestion, DNA extraction, and genotyping. Negative selection of *Palb2* KO embryos was analyzed according to the Hardy–Weinberg equilibrium model, using an online tool (http://ihg.gsf.de/cgi-bin/hw/hwa1.pl). Tetraploid complementation assays were performed as described (53). All experimental procedures involving mouse work were approved by the Dana-Farber Cancer Institute Institutional Care and Use Committee under Animal Protocol 07–011.

Tumorigenesis Studies. Mouse cohorts were monitored for tumor formation biweekly. Mammary tumor formation was scored when a palpable tumor of 1.0 cm in its greatest diameter could be detected, as previously described (27, 30).

Mice harboring tumors were humanely killed when the tumor diameter reached 2.0 cm in its greatest dimension. Mice that were otherwise severely diseased/distressed were also killed according to institutional guidelines. Mantel–Cox logrank test was applied for comparison of tumor-free survival of mouse cohorts.

1. Xia B, et al. (2006) Control of BRCA2 cellular and clinical functions by a nuclear partner, PALB2. *Mol Cell* 22(6):719–729.
2. West SC (2003) Molecular views of recombination proteins and their control. *Nat Rev Mol Cell Biol* 4(6):435–445.
3. Dray E, et al. (2010) Enhancement of RAD51 recombinase activity by the tumor suppressor PALB2. *Nat Struct Mol Biol* 17(10):1255–1259.
4. Buisson R, et al. (2010) Cooperation of breast cancer proteins PALB2 and piccolo BRCA2 in stimulating homologous recombination. *Nat Struct Mol Biol* 17(10):1247–1254.
5. Sy SM, Huen MS, Chen J (2009) PALB2 is an integral component of the BRCA complex required for homologous recombination repair. *Proc Natl Acad Sci USA* 106(17):7155–7160.
6. Zhang F, et al. (2009) PALB2 links BRCA1 and BRCA2 in the DNA-damage response. *Curr Biol* 19(6):524–529.
7. Reid S, et al. (2007) Biallelic mutations in PALB2 cause Fanconi anemia subtype FA-N and predispose to childhood cancer. *Nat Genet* 39(2):162–164.
8. Xia B, et al. (2007) Fanconi anemia is associated with a defect in the BRCA2 partner PALB2. *Nat Genet* 39(2):159–161.
9. Tischkowitz M, et al. (2007) Analysis of PALB2/FANCN-associated breast cancer families. *Proc Natl Acad Sci USA* 104(16):6788–6793.
10. Erkko H, et al. (2007) A recurrent mutation in PALB2 in Finnish cancer families. *Nature* 446(7133):316–319.
11. Jones S, et al. (2009) Exomic sequencing identifies PALB2 as a pancreatic cancer susceptibility gene. *Science* 324(5924):217.
12. Rahman N, et al.; Breast Cancer Susceptibility Collaboration (UK) (2007) PALB2, which encodes a BRCA2-interacting protein, is a breast cancer susceptibility gene. *Nat Genet* 39(2):165–167.
13. Sy SM, Huen MS, Chen J (2009) MRG15 is a novel PALB2-interacting factor involved in homologous recombination. *J Biol Chem* 284(32):21127–21131.
14. Albertson DG, Collins C, McCormick F, Gray JW (2003) Chromosome aberrations in solid tumors. *Nat Genet* 34(4):369–376.
15. Bleuyard JY, Buisson R, Masson JY, Esashi F (2012) ChAM, a novel motif that mediates PALB2 intrinsic chromatin binding and facilitates DNA repair. *EMBO Rep* 13(2):135–141.
16. Huo Y, et al. (2013) Autophagy opposes p53-mediated tumor barrier to facilitate tumorigenesis in a model of PALB2-associated hereditary breast cancer. *Cancer Discovery*, in press.
17. Liu CY, Flesken-Nikitin A, Li S, Zeng Y, Lee WH (1996) Inactivation of the mouse Brca1 gene leads to failure in the morphogenesis of the egg cylinder in early postimplantation development. *Genes Dev* 10(14):1835–1843.
18. Sharan SK, et al. (1997) Embryonic lethality and radiation hypersensitivity mediated by Rad51 in mice lacking Brca2. *Nature* 386(6627):804–810.
19. Rantakari P, et al. (2010) Inactivation of Palb2 gene leads to mesoderm differentiation defect and early embryonic lethality in mice. *Hum Mol Genet* 19(15):3021–3029.
20. Hakem R, et al. (1996) The tumor suppressor gene Brca1 is required for embryonic cellular proliferation in the mouse. *Cell* 85(7):1009–1023.
21. Suzuki A, et al. (1997) Brca2 is required for embryonic cellular proliferation in the mouse. *Genes Dev* 11(10):1242–1252.
22. Bouwman P, et al. (2011) Loss of p53 partially rescues embryonic development of Palb2 knockout mice but does not foster haploinsufficiency of Palb2 in tumour suppression. *J Pathol* 224(1):10–21.
23. Ludwig T, Chapman DL, Papaioannou VE, Efstratiadis A (1997) Targeted mutations of breast cancer susceptibility gene homologs in mice: Lethal phenotypes of Brca1, Brca2, Brca1/Brca2, Brca1/p53, and Brca2/p53 nullizygous embryos. *Genes Dev* 11(10):1226–1241.
24. Hakem R, de la Pompa JL, Elia A, Potter J, Mak TW (1997) Partial rescue of Brca1 (5-6) early embryonic lethality by p53 or p21 null mutation. *Nat Genet* 16(3):298–302.
25. Tallquist MD, Soriano P (2000) Epiblast-restricted Cre expression in MORE mice: A tool to distinguish embryonic vs. extra-embryonic gene function. *Genesis* 26(2):113–115.
26. Dassule HR, Lewis P, Bei M, Maas R, McMahon AP (2000) Sonic hedgehog regulates growth and morphogenesis of the tooth. *Development* 127(22):4775–4785.
27. Jonkers J, et al. (2001) Synergistic tumor suppressor activity of BRCA2 and p53 in a conditional mouse model for breast cancer. *Nat Genet* 29(4):418–425.
28. Erkko H, et al. (2008) Penetrance analysis of the PALB2 c.1592delT founder mutation. *Clin Cancer Res* 14(14):4667–4671.
29. Holstege H, et al. (2009) High incidence of protein-truncating TP53 mutations in BRCA1-related breast cancer. *Cancer Res* 69(8):3625–3633.
30. Liu X, et al. (2007) Somatic loss of BRCA1 and p53 in mice induces mammary tumors with features of human BRCA1-mutated basal-like breast cancer. *Proc Natl Acad Sci USA* 104(29):12111–12116.
31. Loonstra A, et al. (2001) Growth inhibition and DNA damage induced by Cre recombinase in mammalian cells. *Proc Natl Acad Sci USA* 98(16):9209–9214.
32. Molyneux G, et al. (2010) BRCA1 basal-like breast cancers originate from luminal epithelial progenitors and not from basal stem cells. *Cell Stem Cell* 7(3):403–417.
33. Silver DP, Livingston DM (2001) Self-excising retroviral vectors encoding the Cre recombinase overcome Cre-mediated cellular toxicity. *Mol Cell* 8(1):233–243.
34. García MJ, et al. (2009) Analysis of FANCB and FANCN/PALB2 fanconi anemia genes in BRCA1/2-negative Spanish breast cancer families. *Breast Cancer Res Treat* 113(3):545–551.
35. Casadei S, et al. (2011) Contribution of inherited mutations in the BRCA2-interacting protein PALB2 to familial breast cancer. *Cancer Res* 71(6):2222–2229.
36. Xu X, et al. (1999) Conditional mutation of Brca1 in mammary epithelial cells results in blunted ductal morphogenesis and tumour formation. *Nat Genet* 22(1):37–43.
37. Ludwig T, Fisher P, Ganesan S, Efstratiadis A (2001) Tumorigenesis in mice carrying a truncating Brca1 mutation. *Genes Dev* 15(10):1188–1193.
38. Gowen LC, Johnson BL, Latour AM, Sulik KK, Koller BH (1996) Brca1 deficiency results in early embryonic lethality characterized by neuroepithelial abnormalities. *Nat Genet* 12(2):191–194.
39. Cheon DJ, Orsulic S (2011) Mouse models of cancer. *Annu Rev Pathol* 6:95–119.
40. Kallioniemi A, et al. (1992) Comparative genomic hybridization for molecular cytogenetic analysis of solid tumors. *Science* 258(5083):818–821.
41. de Ronde JJ, et al. (2010) KC-SMARTR: An R package for detection of statistically significant aberrations in multi-experiment aCGH data. *BMC Res Notes* 3:298.
42. Cao L, et al. (2009) A selective requirement for 53BP1 in the biological response to genomic instability induced by Brca1 deficiency. *Mol Cell* 35(4):534–541.
43. Bunting SF, et al. (2010) 53BP1 inhibits homologous recombination in Brca1-deficient cells by blocking resection of DNA breaks. *Cell* 141(2):243–254.
44. Bunting SF, et al. (2012) BRCA1 functions independently of homologous recombination in DNA interstrand crosslink repair. *Mol Cell* 46(2):125–135.
45. Bouwman P, et al. (2010) 53BP1 loss rescues BRCA1 deficiency and is associated with triple-negative and BRCA-mutated breast cancers. *Nat Struct Mol Biol* 17(6):688–695.
46. Farmer H, et al. (2005) Targeting the DNA repair defect in BRCA mutant cells as a therapeutic strategy. *Nature* 434(7035):917–921.
47. Brown ET, Holt JT (2009) Rad51 overexpression rescues radiation resistance in BRCA2-defective cancer cells. *Mol Carcinog* 48(2):105–109.
48. Martin RW, et al. (2007) RAD51 up-regulation bypasses BRCA1 function and is a common feature of BRCA1-deficient breast tumors. *Cancer Res* 67(20):9658–9665.
49. Schild D, Wiese C (2010) Overexpression of RAD51 suppresses recombination defects: A possible mechanism to reverse genomic instability. *Nucleic Acids Res* 38(4):1061–1070.
50. Evers B, Jonkers J (2006) Mouse models of BRCA1 and BRCA2 deficiency: Past lessons, current understanding and future prospects. *Oncogene* 25(43):5885–5897.
51. Martins FC, et al. (2012) Evolutionary pathways in BRCA1-associated breast tumors. *Cancer Discov* 2(6):503–511.
52. Kanellopoulou C, et al. (2009) X chromosome inactivation in the absence of Dicer. *Proc Natl Acad Sci USA* 106(4):1122–1127.
53. Nagy A, et al. (1990) Embryonic stem cells alone are able to support fetal development in the mouse. *Development* 110(3):815–821.

GENETICS